Single-Shot Z-Shimmed Sensitivity-Encoded Spiral-In/Out Imaging for fMRI

T-K. Truong[1] and A. W. Song[1]

[1]Brain Imaging and Analysis Center, Duke University, Durham, NC, United States

Introduction

BOLD fMRI can be severely hampered by signal loss due to static magnetic field (B_0) inhomogeneities near air/tissue interfaces, especially at high field. An effective method to correct for such artifacts is z-shimming, in which multiple images are acquired with different gradients applied to compensate for the susceptibility-induced gradients, and then combined to achieve a uniform signal recovery. However, implementations requiring separate acquisitions are not efficient, whereas single-shot multiecho implementations use images acquired with different BOLD contrasts, neither of which is suitable for fMRI. Guo *et al*. [1] therefore implemented z-shimming in a single-shot spiral-in/out sequence by adding a z-shim gradient between the two acquisitions with nearly identical TEs. Despite promising results, this technique has several limitations, which we address as follows.

1) A z-shim gradient was used only for the spiral-out acquisition, which may not be optimal for complex B_0 inhomogeneities such as those existing in inferior brain regions. Here, we add a second z-shim gradient before the spiral-in acquisition (**Fig. 1**) and optimize both gradients to achieve the most uniform signal recovery.

2) The same z-shim gradient was used for all slices, resulting in a substantial variation of its effectiveness across the imaged slab as well as a reduction of SNR in homogeneous slices. Here, we optimize the z-shim gradients slice-by-slice and turn them off when appropriate.

3) The optimal z-shim gradient was determined empirically by successively trying different values, which is impractical. Here, we acquire a B_0 map to efficiently (< 1 min) and accurately optimize the z-shim gradients.

4) The global signal loss due to T_2^* relaxation limited the readout duration, and hence the spatial resolution. Here, we use SENSE parallel imaging to double the in-plane resolution while maintaining a limited readout duration and a high temporal resolution. Moreover, the signal loss due to in-plane susceptibility-induced gradients is reduced, thus complementing the z-shimming, which only compensates for through-plane gradients.

Methods

The susceptibility-induced gradient in the slice direction causes a phase dispersion $\phi_{susc}(z) = \gamma\,(\partial B_0/\partial z)\,z\,TE$ for $-\Delta z/2 \le z \le \Delta z/2$, assuming a linear gradient and where γ is the gyromagnetic ratio and Δz the slice thickness. This intravoxel dephasing results in a signal loss $\eta \equiv S/S_0 = \mathrm{sinc}[\phi_{susc}(\Delta z)/2]$, assuming a rectangular slice profile and a uniform spin density across the slice. A z-shim gradient of amplitude G and duration T causes an additional phase dispersion $\phi_{z\text{-}shim}(z) = \gamma\,G\,T\,z$, so that $\eta = \mathrm{sinc}\{[\phi_{susc}(\Delta z) + \phi_{z\text{-}shim}(\Delta z)]/2\}$. The signal is thus fully recovered where $\phi_{z\text{-}shim} = -\phi_{susc}$. In this work, the spiral-in/out images are combined by square root of the sum of squares, so that $\eta_{in/out} = \mathrm{sqrt}[(\eta_{in}^2 + \eta_{out}^2)/2]$. The optimal z-shim gradients yielding the most uniform signal recovery are determined by minimizing the standard deviation of $\eta_{in/out}$ inside the sample normalized to its mean.

Spiral SENSE images are acquired by reducing the radial k-space sampling density, and reconstructed using an iterative conjugate gradient algorithm [2] and a least squares nonuniform FFT gridding method [3]. A B_0 map is acquired using a multiecho spin echo sequence, wherein a train of gradient echo images are acquired before and after the spin echo, and computed by pixel-wise linear regression of the unwrapped phase images [4].

The studies were performed at 3 T using an 8-channel RF coil. A spherical water phantom containing a ping-pong ball was designed to simulate an air cavity inside a human head. The flat air/water interface at the top induced additional B_0 inhomogeneities. Axial spiral-in/out images were acquired using TR 1.5 s, TE 46/47 ms, flip angle 60°, FOV 16 cm, matrix 128×128, Δz 2.5 mm, and a SENSE reduction factor of 2. $\phi_{z\text{-}shim}(\Delta z)$ values of 0°, ±90°, ±180°, ±270°, and ±360° were used for both the spiral-in and spiral-out acquisitions, and each pair of images combined, but only to validate (not calibrate) the sequence. Two volunteers who provided informed consent were studied using TR 2 s, TE 38/39 ms, FOV 24 cm, Δz 3.8 mm, and otherwise identical parameters.

Results and Discussion

A map of $\phi_{susc}(\Delta z)$ of the phantom (**Fig. 2**) shows regions with positive or negative susceptibility-induced phase shifts. The resulting maps of η_{in}, η_{out}, and $\eta_{in/out}$ (**Fig. 3**) show signal loss in these regions when no z-shimming is applied. The signal can be effectively recovered by using either $\phi_{z\text{-}shim,in}(\Delta z) = 180°$ or $\phi_{z\text{-}shim,out}(\Delta z) = -180°$, but only in one region. Both z-shim gradients are required to achieve the most uniform signal recovery. The acquired spiral-in, spiral-out, and combined images (**Fig. 4**) confirm these predictions, even though they are not exactly identical to the maps shown in Fig. 3, since the latter do not take into account the T_2^* filtering of the spiral-in and spiral-out trajectories. In particular, the spiral-in images are less affected by susceptibility-induced signal loss, but show an artifactual localized signal increase, which can also be corrected for with z-shimming.

The human $\phi_{susc}(\Delta z)$ map (**Fig. 5**) shows positive and negative susceptibility-induced phase shifts in the inferior frontal and temporal lobes near the sinuses and ear canals, respectively. As for the phantom, the optimal z-shim gradients were determined to be $\phi_{z\text{-}shim,in}(\Delta z) = 180°$ and $\phi_{z\text{-}shim,out}(\Delta z) = -180°$ from maps of the estimated signal loss $\eta_{in/out}$. The acquired images (**Fig. 6**) show artifactual signal loss and/or increase in these regions, which can only be simultaneously corrected for when both z-shim gradients are used.

In conclusion, our improved single-shot z-shimmed spiral-in/out sequence can effectively and efficiently correct for susceptibility artifacts in high-resolution SENSE images. Studies are currently underway to demonstrate these advantages in fMRI applications.

References: [1] Guo *et al*. JMRI 2003;18:389–395. [2] Pruessmann *et al*. MRM 2001;46:638–651. [3] Sha *et al*. JMR 2003;162:250–258. [4] Chen *et al*. Neuroimage 2006;30:121–129. This work was supported by NIH grants NS 41328 and NS 50329.

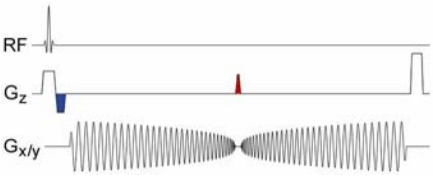

Fig. 1: Single-shot spiral-in/out sequence with z-shim gradients applied before the spiral-in (in blue, combined with the slice-select rephaser) and between the spiral-in and spiral-out acquisitions (in red, combined with the rephaser of the first z-shim gradient).

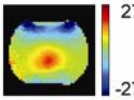

Fig. 2: Susceptibility-induced phase shift $\phi_{susc}(\Delta z)$.

Fig. 3: Estimated signal loss η_{in}, η_{out}, and $\eta_{in/out}$ for different $\phi_{z\text{-}shim}(\Delta z)$.

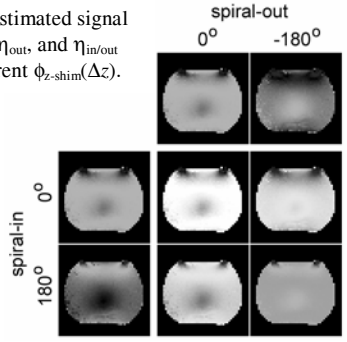

Fig. 4: Spiral-in, spiral-out, and combined images acquired with different $\phi_{z\text{-}shim}(\Delta z)$.

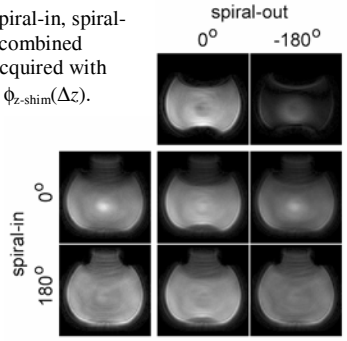

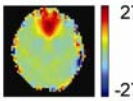

Fig. 5: Susceptibility-induced phase shift $\phi_{susc}(\Delta z)$.

Fig. 6: Spiral-in, spiral-out, and combined images acquired with different $\phi_{z\text{-}shim}(\Delta z)$.